

Conditional purity and quantum correlation measures in two qubit mixed states

L. Rebón,^{1,2,*} R. Rossignoli,¹ J.J.M. Varga,³ N. Gigena,¹ N. Canosa,¹ C. Iemmi,³ and S. Ledesma³

¹*Departamento de Física, Instituto de Física de La Plata-CONICET, Universidad Nacional de La Plata, C.C. 67, 1900 La Plata, Argentina*

²*Institut für Gravitationsphysik, Leibniz Universität Hannover and Max-Planck-Institut für Gravitationsphysik (Albert-Einstein-Institut), Callinstrasse 38, 30167 Hannover, Germany*

³*Departamento de Física, FCEyN, Universidad de Buenos Aires-CONICET, Buenos Aires 1428, Argentina*

(Dated: March 7, 2019)

We analyze and show experimental results of the conditional purity, the quantum discord and other related measures of quantum correlation in mixed two-qubit states constructed from a pair of photons in identical polarization states. The considered states are relevant for the description of spin pair states in interacting spin chains in a transverse magnetic field. We derive clean analytical expressions for the conditional local purity and other correlation measures obtained as a result of a remote local projective measurement, which are fully verified by the experimental results. A simple exact expression for the quantum discord of these states in terms of the maximum conditional purity is also derived.

PACS numbers: 03.67.-a, 03.65.Ud, 03.65.Ta, 42.50.Ex

I. INTRODUCTION

Quantum correlations are at the heart of quantum information theory, constituting one of the key features that distinguishes quantum from classical composite systems. They are recognized as the essential resource that enables several quantum information processing schemes [1], such as quantum teleportation [2] and quantum algorithms exhibiting an exponential speed-up over their classical counterparts [3, 4]. Although quantum entanglement [5, 6] is the strongest type of quantum correlations, it does not encompass all non-classical correlations that can be exhibited by mixed states of composite systems. For such states, several other measures of quantum-like correlations have been proposed [7], with quantum discord [8–11] and information deficit [12, 13] playing a prominent role. In fact, the presence of discord-like correlations have been shown to be important for quantum state discrimination [14], quantum cryptography [15] and quantum metrology [16].

Quantum discord for a bipartite system can be defined [8] through the difference between two distinct quantum generalizations of the classical conditional von Neumann entropy, one being the standard formal extension of the classical expression while the other one, introduced in [8], involves a local measurement on one of the constituents. The latter generalization measures the average conditional mixedness of the unmeasured component (A) after the local measurement on the other component (B) and is always a positive quantity, which is smaller or at least never larger than the original marginal entropy $S(A)$. This conditional entropy, which depends on the choice of the local measurement, has been recently extended to more general entropic forms [17]. In particular, this gen-

eralization allows the use of simpler entropies, which can be more easily evaluated and enable a clean analytical solution of the associated optimization problem (i.e., that of selecting the local measurement which minimizes the conditional entropy) in general qudit-qubit states. Such entropies can also be directly related to the purity, an experimentally accessible quantity which does not require a full state tomography [18, 19].

The aim of this work is to analyze and experimentally obtain the conditional purity, the quantum discord and other related measures of discord-like correlations [13, 20] in a particular class of mixed states which can be faithfully simulated through photonic quantum systems and linear optics [21, 22]. These states, which are mixtures of non-orthogonal aligned states, arise naturally in different contexts, in particular as reduced pair states in the exact ground state of spin 1/2 chains and arrays with XY or XYZ couplings, in the immediate vicinity of the factorizing magnetic field [23–25]. In these chains they can also provide a basic description of reduced pair states in mean-field symmetry- breaking phases ($B < B_c$) [26].

For such states, described in sections II A–II B, we first derive in II C–II D simple analytical expressions for the conditional reduced state and its purity after a local measurement on one of the qubits, including the average conditional purity and its maximum among all possible local projective measurements. We then derive in sec. II E a simple closed analytical expression for the quantum discord of these states in terms of the maximum conditional purity, which is also verified numerically. Additionally, in II F we present expressions for the global post-measurement purity and its minimizing measurement, which allows to evaluate the associated information deficit and the geometric discord. These quantities are also analyzed and compared. We have then experimentally tested these theoretical results using polarization-encoded photonic qubits that arise from a source emitting a pair of photons in the same polarization state,

*Electronic address: lorena.rebon@aei.mpg.de

which enables to reproduce the mixed two qubit states. A description of the experimental setup used to prepare the desired state and perform the local measurements is given at the beginning of section III A, with III B devoted to present the experimental results and their comparison with the theoretical predictions. Conclusions are finally given in IV.

II. THEORY

A. Initial state

We consider the symmetric two qubit mixed state

$$\rho_{AB} = p|\theta\theta\rangle\langle\theta\theta| + q|-\theta-\theta\rangle\langle-\theta-\theta|, \quad (1)$$

where $|\theta\theta\rangle\langle\theta\theta| \equiv |\theta\rangle\langle\theta| \otimes |\theta\rangle\langle\theta|$ with

$$|\pm\theta\rangle = \cos\frac{\theta}{2}|0\rangle \pm \sin\frac{\theta}{2}|1\rangle, \quad (2)$$

pure single qubit states forming angles $\pm\theta$ with the z axis on the Bloch sphere ($\langle\theta|\boldsymbol{\sigma}|\theta\rangle = (\sin\theta, 0, \cos\theta)$, being $\boldsymbol{\sigma} = (\sigma_x, \sigma_y, \sigma_z)$ the Pauli matrices), and $p \in [0, 1]$, $q = 1 - p$ are the probabilities of preparing both qubits in the states $|\theta\rangle$ and $|-\theta\rangle$ respectively. Without loss of generality we can restrict θ to the interval $[0, \pi/2]$ and assume $p \geq q$. Any rank 2 mixture of the form $\rho_{AB} = p|\Omega\Omega\rangle\langle\Omega\Omega| + q|\Omega'\Omega'\rangle\langle\Omega'\Omega'|$, with $|\Omega\rangle = \cos\frac{\theta}{2}|0\rangle + e^{i\phi}\sin\frac{\theta}{2}|1\rangle$ a general two-qubit state, can be rewritten at once in the form (1) by choosing a new z axis in the Bloch sphere halfway between the directions $\Omega = (\theta, \phi)$ and $\Omega' = (\theta', \phi')$, with the x axis in the plane determined by them. And a mixture $\rho_{AB} = p|\Omega_1\Omega_2\rangle\langle\Omega_1\Omega_2| + q|\Omega'_1\Omega'_2\rangle\langle\Omega'_1\Omega'_2|$, where the angle between Ω'_2 and Ω_2 is identical with that between Ω'_1 and Ω_1 , can be also brought to the form (1) by applying local rotations on one of the qubits that shift Ω_2 to Ω_1 and Ω'_2 to Ω'_1 . These local rotations will not affect correlation measures.

Mixed states of the form (1) arise often in different contexts. For instance, they can emerge naturally as reduced two-spin states in the ground state of ferromagnetic-type spin 1/2 chains or arrays with anisotropic XY or XYZ couplings in the immediate vicinity of the transverse factorizing magnetic field [24–27]. At this point the exact ground state of the spin system becomes two-fold degenerate, being an arbitrary linear combination of uniform completely separable states:

$$|GS\rangle = \alpha|\theta\theta\dots\rangle + \beta|-\theta-\theta\dots\rangle, \quad (3)$$

where $|\alpha|^2 + |\beta|^2 = 1$ and θ is determined by the coupling anisotropy [24] (assumed constant for all coupled pairs). The state (3) leads to the reduced state (1) with $p = |\alpha|^2$, $q = |\beta|^2$ for *any* pair $i \neq j$, after tracing out the complementary qubits and neglecting the complementary overlap $\langle-\theta|\theta\rangle^{n-2} = \cos^{n-2}\theta$, which decreases exponentially with increasing n if $|\cos\theta| < 1$.

In particular, as the transverse factorizing field is approached, the exact ground state approaches as side-limits the orthogonal definite spin parity combinations $|GS_{\pm}\rangle$ obtained for $\beta = \pm\alpha$ [26], which lead to $p = q = 1/2$. An identical reduced state will be approached at low temperatures, since the thermal canonical state will become a uniform mixture $\frac{1}{2}\sum_{\nu=\pm}|GS_{\nu}\rangle\langle GS_{\nu}|$ of the degenerate definite parity ground states. In fact, any statistical mixture of ground states (3) will also lead to a reduced state of the form (1) if $\langle-\theta|\theta\rangle^{n-2}$ is neglected. And in the mean field approximation for these chains [26, 27], a reduced state of the form (1) with $p = q = 1/2$ naturally arises in the whole parity breaking phase after parity symmetry restoration [26, 27], becoming exact at the factorizing point.

We should remark that these considerations also apply to antiferromagnetic-type XYZ chains in the vicinity of factorizing points [23]. In this case the reduced states of contiguous pairs will rather be of the form $\rho_{AB} = p|\theta_1\theta_2\rangle\langle\theta_1\theta_2| + q|\theta_2\theta_1\rangle\langle\theta_2\theta_1|$, but as stated before, such state can be rewritten in the form (1) with $\theta = |\theta_1 - \theta_2|/2$ after applying local rotations.

The states (1) can be simulated using a source emitting a pair of photons in the same polarization state, e.g. by spontaneous parametric down-conversion (SPDC) produced in nonlinear crystal cut for type I phase matching [28, 29] and linear optics, such that

$$|\pm\theta\rangle = \cos\frac{\theta}{2}|V\rangle \pm \sin\frac{\theta}{2}|H\rangle \quad (4)$$

are linearly polarized states at angles $\pm\theta/2$ with the vertical direction. Here $|V\rangle \equiv |0\rangle$, $|H\rangle \equiv |1\rangle$ denote the orthogonal linearly polarized states in the vertical and horizontal directions respectively.

B. Purity and basic properties

Since the states $|\pm\theta\rangle$ are not orthogonal for $\theta < \pi/2$, the purity of the state (1),

$$P_{AB} = \text{Tr } \rho_{AB}^2 = 1 - 2pq(1 - \cos^4\theta), \quad (5)$$

is higher than that of a mixture of orthogonal states (given by $1 - 2pq$). Eq. (5) is an increasing function of the overlap $|\langle-\theta|\theta\rangle| = |\cos\theta|$, reaching its maximum 1 if and only if (iff) $\theta = 0$ or $pq = 0$, i.e. iff ρ_{AB} is pure ($\rho_{AB}^2 = \rho_{AB}$). The purity (5) determines the two non-zero eigenvalues of (1),

$$\lambda_{AB}^{\pm} = \frac{1}{2}[1 \pm \sqrt{2P_{AB} - 1}], \quad (6)$$

and hence, the value of any entropy

$$S_f(\rho_{AB}) = \text{Tr } f(\rho_{AB}) = f(\lambda_+) + f(\lambda_-), \quad (7)$$

where f is a concave function satisfying $f(0) = f(1) = 0$ [30, 31]. The von Neumann entropy $S(\rho)$ corresponds

to $f(\rho) = -\rho \log_2 \rho$, while the linear entropy $S_2(\rho)$ to $f(\rho) = -2\rho(1 - \rho)$:

$$S_2(\rho_{AB}) = 2(1 - \text{Tr} \rho_{AB}^2) = 2(1 - P_{AB}), \quad (8)$$

which is just a linear decreasing function of P_{AB} . All entropies (7) will be decreasing functions of P_{AB} , vanishing iff $P_{AB} = 1$.

The state (1) is *separable*, i.e., a convex mixture of product states [6]. Nonetheless, it is not classically correlated if $\theta \in (0, \pi/2)$ and $pq \neq 0$, since in this case it is not diagonal in an orthogonal product basis. It will then be affected by any local measurement, having a finite quantum discord, as discussed in sec. II E. Accordingly, it has entangled eigenstates, of the form $|\Psi_{AB}^\pm\rangle = \alpha_\pm \frac{\cos^2 \frac{\theta}{2} |00\rangle + \sin^2 \frac{\theta}{2} |11\rangle}{\sqrt{1 - \frac{1}{2} \sin^2 \theta}} + \beta_\pm \frac{|01\rangle + |10\rangle}{\sqrt{2}}$ for λ_{AB}^\pm , which depend on θ and p .

The reduced state of each of the qubits (or photons) is

$$\rho_A = \text{Tr}_B \rho_{AB} = p|\theta\rangle\langle\theta| + q|-\theta\rangle\langle-\theta| \quad (9)$$

$$= \frac{1}{2} \begin{pmatrix} 1 + \cos \theta & (p - q) \sin \theta \\ (p - q) \sin \theta & 1 - \cos \theta \end{pmatrix}, \quad (10)$$

where (10) is the representation in the standard basis $\{|V\rangle, |H\rangle\}$. It corresponds to a Bloch vector $\mathbf{r}_A = \text{Tr} \rho_A \boldsymbol{\sigma} = ((p - q) \sin \theta, 0, \cos \theta)$. The *local* purity is then

$$P_A = \text{Tr} \rho_A^2 = 1 - 2pq \sin^2 \theta, \quad (11)$$

and the eigenvalues of ρ_A are

$$\lambda_A^\pm = (1 \pm \sqrt{2P_A - 1})/2 \quad (12)$$

being verified that $P_A \geq P_{AB}$, $\lambda_A^+ \geq \lambda_{AB}^+$, in agreement with the general majorization property [32] $\rho_A \prec \rho_{AB}$ valid for *any* separable mixed state ρ_{AB} [33, 34].

C. Conditional local state and purity after remote local measurement

Let us consider now a projective polarization measurement on photon B , defined by the orthogonal projectors

$$\Pi_+ = |\phi\rangle\langle\phi|, \quad \Pi_- = |\phi + \pi\rangle\langle\phi + \pi|, \quad (13)$$

where $|\phi\rangle = \cos \frac{\phi}{2} |V\rangle + \sin \frac{\phi}{2} |H\rangle$, $|\phi + \pi\rangle = -\sin \frac{\phi}{2} |V\rangle + \cos \frac{\phi}{2} |H\rangle$ and $\Pi_+ + \Pi_- = 1$. This means projecting onto linearly polarized states at angles $\phi/2$ and $\phi/2 + \pi/2$ respectively. The probability of obtaining result $+$ ($\phi/2$) or $-$ ($\phi/2 + \pi/2$) is

$$\begin{aligned} r_\pm &= \text{Tr} (\rho_{AB} I_A \otimes \Pi_\pm) \\ &= \frac{1}{2} [1 \pm p \cos(\phi - \theta) \pm q \cos(\phi + \theta)]. \end{aligned} \quad (14)$$

Obviously a $+$ result for angle ϕ is equivalent to a $-$ result for angle $\phi \pm \pi$. As a function of ϕ , r_\pm is extremum for

$$\tan \phi = (p - q) \tan \theta, \quad (15)$$

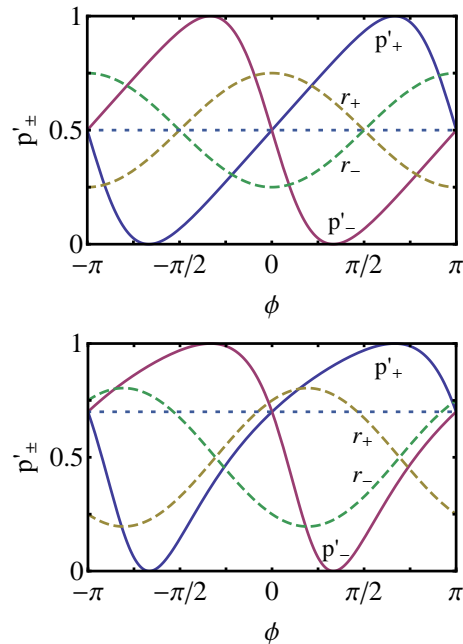


FIG. 1: (Color online) The probabilities p'_\pm , Eq. (17), of the conditional reduced states (16) of A after a measurement with result \pm at B along angle ϕ , for $\theta = \pi/3$ and initial values $p = 0.5$ (top) and $p = 0.7$ (bottom), indicated by the horizontal dotted lines. It is seen that p'_\pm cover all values between 0 and 1, with $p'_+ = 1$ at $\phi = \pi - \theta$ and 0 at $\phi = \theta - \pi$, while $p'_- = 0$ at $\phi = \theta$ and 1 at $\phi = -\theta$. The dashed lines depict the probabilities r_\pm , Eq. (14), of obtaining result \pm at B .

with r_+ maximum for ϕ between 0 and θ if $p \geq q$, as seen in Fig. 1.

After a measurement at B with known result, the post-measurement state of the unmeasured photon will have again the form (9), but with modified probabilities p'_\pm, q'_\pm , which depend on both the measurement angle ϕ and measurement result \pm :

$$\begin{aligned} \rho_{A/B_\pm} &= r_\pm^{-1} \text{Tr}_B (\rho_{AB} I_A \otimes \Pi_\pm) \\ &= p'_\pm |\theta\rangle\langle\theta| + q'_\pm |-\theta\rangle\langle-\theta|, \end{aligned} \quad (16)$$

with

$$\begin{aligned} p'_\pm &= p \frac{1 \pm \cos(\theta - \phi)}{2r_\pm} \\ q'_\pm &= q \frac{1 \pm \cos(\theta + \phi)}{2r_\pm} = 1 - p'_\pm. \end{aligned} \quad (17)$$

It is verified that $r_+ \rho_{A/B_+} + r_- \rho_{A/B_-} = \rho_A$, i.e., that the average post-measurement state at A is unchanged. It is also seen that if $\phi = 0$, $p'_\pm = p$, i.e., $\rho_{A/B_\pm} = \rho_A$ irrespective of the values of θ , p and the result of the measurement. Such measurement then leaves the marginal state of the unmeasured photon (but not the whole ρ_{AB}) unchanged. This invariance will not occur for other values of ϕ .

As seen in Fig. 1, the new probabilities p'_\pm cover all possible values from 0 to 1 as the measurement angle ϕ

is varied. For $p > q$, p'_+ (p'_-) stays above (below) the initial value p for $\phi \geq 0$, and the opposite behavior takes place for $\phi \leq 0$. The purities of the states (16) are given by

$$\begin{aligned} P_{A/B_{\pm}} &= 1 - 2p'q' \sin^2 \theta \\ &= 1 - 2pq \frac{[1 \pm \cos(\theta - \phi)][1 \pm \cos(\theta + \phi)]}{4r_{\pm}^2} \sin^2 \theta, \end{aligned} \quad (18)$$

and can then be *larger or smaller* than the original purity (11), satisfying

$$1 - \frac{1}{2} \sin^2 \theta \leq P_{A/B_{\pm}} \leq 1. \quad (19)$$

For P_{A/B_-} , the upper limit is always reached if $\phi = \pm\theta$, as in this case a $-$ result implies with certainty a pure post-measurement state $|\mp\theta\rangle$ in A , i.e., $p'_- = 0$ or 1 , as verified in Fig. 1. Such result has probability $r_- = q \sin^2 \theta$ ($p \sin^2 \theta$) if $\phi = \theta$ ($-\theta$). The same occurs for P_{A/B_+} if $\phi = \mp(\pi - \theta)$. On the other hand, the lower limit in (18) corresponds to $p'_{\pm} = 1/2$ and can be reached for angles ϕ satisfying

$$\tan \phi = \frac{(p - q) \sin \theta}{\cos \theta \pm 2\sqrt{pq}}, \quad (20)$$

in which case $p'_- = 1/2$ for the roots of (20) satisfying $\phi \geq 0$ while $p'_+ = 1/2$ for those satisfying $\phi \leq 0$, as seen in Fig. 1. Hence by suitable measurements and results at B it is always possible to have the post-measurement state at A *pure* or also “*equilibrated*”, i.e., with equal weights of both states of the mixture.

D. Average conditional purity

The *average* conditional purity of A after the previous measurement at B is given by

$$\begin{aligned} P_{A/B_{\phi}} &= r_+ P_{A/B_+} + r_- P_{A/B_-} \\ &= 1 - 2pq\gamma \sin^2 \theta, \end{aligned} \quad (21)$$

where

$$\begin{aligned} \gamma &= \frac{r_+ p'_+ q'_+ + r_- p'_- q'_-}{pq} \\ &= \frac{p \sin^2(\theta - \phi) + q \sin^2(\theta + \phi)}{1 - [p \cos(\theta - \phi) + q \cos(\theta + \phi)]^2} \leq 1. \end{aligned} \quad (22)$$

Hence, in contrast with $P_{A/B_{\pm}}$, $P_{A/B_{\phi}}$ is never lower than the original purity:

$$P_{A/B_{\phi}} \geq P_A, \quad (23)$$

in agreement with the general results of [17]. Eq. (21) is in fact linearly related to the measurement dependent S_2 conditional entropy [17], which becomes here

$$\begin{aligned} S_2(A/B_{\phi}) &= r_+ S_2(\rho_{A/B_+}) + r_- S_2(\rho_{A/B_-}) \\ &= 2(1 - P_{A/B_{\phi}}) = 4pq\gamma \sin^2 \theta, \end{aligned} \quad (24)$$

and is never greater than the original local entropy $S_2(\rho_A) = 4pq \sin^2 \theta$.

The difference $P_{A/B_{\phi}} - P_A = 2pq(1 - \gamma) \sin^2 \theta$ is the average purity gain at A due to the local measurement at B , and depends on the measurement angle ϕ . While it always vanishes for $\phi = 0$, where $\gamma = 1$, it is otherwise positive. Its *maximum* is attained for

$$\tan \phi = \frac{\tan \theta}{p - q}, \quad (25)$$

in which case $\gamma = \cos^2 \theta$, leading to

$$P_{A/B} \equiv \text{Max}_{\phi} P_{A/B_{\phi}} = 1 - 2pq \sin^2 \theta \cos^2 \theta. \quad (26)$$

Moreover, at this point $p'_+ = q'_-$ and hence,

$$P_{A/B_+} = P_{A/B_-} = P_{A/B}, \quad (27)$$

so that the maximum average gain is attained at an angle where the post-measurement local purity (but not the local state) is *independent* of the result of the measurement (see also Fig. 4) in sec. III B.

The maximum average purity gain is thus $2pq \sin^4 \theta$. The maximum average conditional purity (26) has a deep significance. The associated minimum S_2 conditional entropy

$$S_2(A/B) = \text{Min}_{\phi} S_2(A|B_{\phi}) = 2(1 - P_{A/B}) = pq \sin^2 2\theta, \quad (28)$$

represents the *squared concurrence* [35] between A and a third system C purifying the whole system ABC [17, 36, 37]. C can be here chosen as a single qubit due to the rank 2 of ρ_{AB} . As a consequence (see next subsection), the maximum average conditional purity (26) will also determine the *quantum discord* of the state (1), enabling a simple analytical expression for the latter. The behavior of $P_{A/B}$ as a function of the “aperture” angle θ of the state (1) is depicted on Fig. 2. where it is seen that it reaches its maximum 1 just for $\theta = 0$ or $\pi/2$, i.e., when the state (1) is either a product state ($\theta = 0$) or a classically correlated state ($\theta = \pi/2$), i.e., a state of zero discord in both cases.

The maximizing ϕ determined by (25) differs from $\pm\theta$ if $\theta > 0$, $pq > 0$, as seen in the bottom panel of Fig. 2. It satisfies $\phi \geq \theta$ if $p \geq q$, with $\phi \rightarrow \theta$ for $p \rightarrow 1$, where

$$\phi \approx \theta + (1 - p) \sin 2\theta,$$

but $\phi \rightarrow \pi/2$ for $p \rightarrow 1/2$ and $\theta \neq 0$, in which case

$$\phi \approx \frac{\pi}{2} - 2(p - \frac{1}{2}) / \tan \theta.$$

Hence, for $p = q$ it becomes *independent* of θ , preferring always a measurement along the x axis in the Bloch sphere (i.e., projecting onto linearly polarized states at angles $\pm\pi/4$).

The previous feature is in agreement with the general considerations of [17]. The maximizing measurement direction \mathbf{k} in the Bloch sphere is essentially that of maximum correlation. It satisfies the generalized eigenvalue equation [17]

$$C^T C \mathbf{k} = \lambda N_B \mathbf{k} \quad (29)$$

with λ the largest eigenvalue, where C is the correlation tensor of the system, of elements

$$C_{\mu\nu} = \langle \sigma_\mu^A \otimes \sigma_\nu^B \rangle - \langle \sigma_\mu^A \rangle \langle \sigma_\nu^B \rangle, \quad (30)$$

and $N_B = I_3 - \mathbf{r}_B \mathbf{r}_B^T$, with $\mathbf{r}_B = \langle \sigma^B \rangle$ the original Bloch vector of qubit B . Here $\mathbf{r}_A = \mathbf{r}_B = ((p-q) \sin \theta, 0, \cos \theta)$ and

$$C_{\mu\nu} = \delta_{\mu\nu} \delta_{\mu x} 4pq \sin^2 \theta, \quad (31)$$

so that correlations arise just along the x direction. Eq. (29) then leads to a minimizing \mathbf{k} in the xz plane, i.e., $\mathbf{k} = (\sin \phi, 0, \cos \phi)$, with ϕ satisfying Eq. (25). And for $p = q$, \mathbf{k} becomes parallel to the x axis as N_B becomes diagonal.

Let us also remark that the correlation tensor C determines the set of post-measurement states of A after a local measurement at B [17]. In terms of C and the Bloch vectors of the marginal states \mathbf{r}_A and \mathbf{r}_B , the vector representing the conditional state of qubit A after a measurement on qubit B along the direction of the vector \mathbf{k} with result \pm is given by [17]

$$\mathbf{r}_{A/\pm \mathbf{k}} = \mathbf{r}_A \pm \frac{C \mathbf{k}}{1 \pm \mathbf{r}_B \cdot \mathbf{k}}. \quad (32)$$

Since $\pm \mathbf{k}$ is any point on the Bloch sphere of qubit B , the vectors $\tilde{\mathbf{k}}_\pm = \pm \mathbf{k} / (1 \pm \mathbf{r}_B \cdot \mathbf{k})$ are points on the surface of an ellipsoid with eccentricity \mathbf{r}_B with the origin as one of its foci. The correlation tensor C then maps this ellipsoid into another ellipsoid inside the Bloch sphere of A if C has rank 3, an ellipse if it has rank 2, and a *needle* if it has rank 1, which is the case of the state (1). Such needle is here the straight line in the Bloch sphere of A connecting the states $|\theta\rangle$ and $|\!-\!\theta\rangle$. Needle states include also zero discord states, i.e., classically correlated as well as one-way classical states. However, in the latter the correlation tensor can be taken, after suitable local rotations, to the form $C_{\mu\nu} \propto \delta_{\mu\nu} \delta_{\mu z}$ with z the direction of the local Bloch vector \mathbf{r}_B , which is not the case of (31) if $\theta \in (0, \pi/2)$ and $pq \neq 0$.

E. Quantum Discord

As previously mentioned, the state (1) is separable but not classically correlated for $\theta \in (0, \pi)$ and $pq \neq 0$, having in this case a finite *Quantum Discord* [8, 9]. As a function of the measurement angle, this quantity can be evaluated as the minimum of the difference

$$D(A/B_\phi) = S(A|B_\phi) - S(A|B), \quad (33)$$

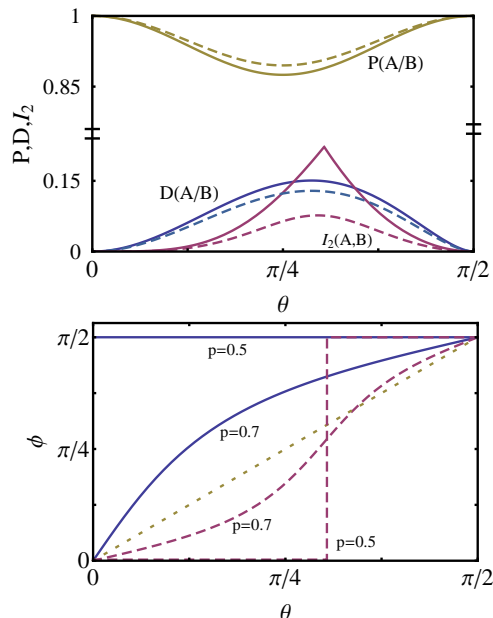


FIG. 2: (Color online) Top: The maximum average conditional purity $P(A/B) \equiv P_{A/B}$, Eq. (26), together with the quantum discord, Eq. (36) and the minimum global purity difference, Eq. (43), as a function of the aperture angle θ of the state (1) for $p = 0.5$ (solid lines) and $p = 0.7$ (dashed lines). Bottom: The measurement angles which maximize the average conditional purity (21) (solid lines, Eq. (25)) and the global post-measurement purity (39) (dashed lines, Eq. (44)), as a function of the aperture angle θ for $p = 0.5$ and $p = 0.7$. The dotted line depicts θ for reference. For $p = 0.5$, the angle maximizing (39) undergoes a sharp $0 \rightarrow \pi/2$ transition at $\theta = \arccos 1/\sqrt{3}$, which originates the sharp peak in I_2 seen in the top panel and which becomes smoothed out for $p > 1/2$. The angle minimizing the quantum discord (33) coincides here exactly with that maximizing the conditional purity (21) (see text).

where $S(A|B) = S(\rho_{AB}) - S(\rho_B)$ is the standard von Neumann conditional entropy [30] and

$$S(A|B_\phi) = r_+ S(\rho_{A/B_+}) + r_- S(\rho_{A/B_-}) \quad (34)$$

the measurement dependent von Neumann conditional entropy [8] (i.e., the von Neumann-based version of Eq. (24)). Here $S(A|B)$ can be calculated with the eigenvalues $\lambda_{AB}^\pm, \lambda_A^\pm$ of ρ_{AB} and ρ_A , Eqs. (6), (12), while $S(A|B_\phi)$ requires those of the conditional states (16), given by $\lambda_{A/B_\nu}^\pm = (1 \pm \sqrt{2P_{A/B_\nu} - 1})/2$ for $\nu = \pm$. Hence, all quantities can be evaluated with the purities P_{AB} , P_A and P_{A/B_\pm} .

The actual quantum discord is the minimum over ϕ of Eq. (33) [8, 11]:

$$D(A/B) = \text{Min}_\phi D(A/B_\phi). \quad (35)$$

The minimization should in principle be extended to general POVM measurements, but in the present case of a

rank 2 state, it is sufficient to consider just projective measurements, which for the present case can be reduced to a measurement in the xz plane. Furthermore, the minimum (35) can be here evaluated *analytically*: The minimizing measurement angle ϕ is *exactly that which maximizes the average conditional purity*, determined by Eq. (25), and the ensuing minimum (35) is a *decreasing function of the maximum average conditional purity* (26) (even though for general ϕ (33) is not a direct function of (21)). We obtain

$$D(A/B) = -f_+ \log_2 f_+ - f_- \log_2 f_- - S(A|B) \quad (36)$$

where

$$f_{\pm} = \frac{1 \pm \sqrt{2P_{A/B} - 1}}{2}. \quad (37)$$

Proof: According to the result of [36], the minimum of $S(A|B_{\phi})$ is the entanglement of formation between A and a closing third system C purifying the whole system, which as stated before, can be chosen here as a single qubit. But in such a case this entanglement is determined by the concurrence between A and C through the expression of [35], whose square C_{AC}^2 is just the minimum S_2 conditional entropy (24) of A given a measurement at B . This entails that the minimum $S(A|B_{\phi})$ is given by the first two terms in (36), since $2P_{A/B} - 1 = 1 - C_{AC}^2$. We have also checked this result numerically.

For $\theta = 0$ (ρ_{AB} product state) or $\theta = \pi/2$ (ρ_{AB} classically correlated), $P_{A/B} = 1$ and consequently $D(A/B) = 0$. Otherwise $P_{A/B} < 1$ and $D(A/B) > 0$, as appreciated in Fig. 2. Note, however, that as a function of θ , $P_{A/B}$ is minimum at $\pi/4$ (Eq. (26)), while $D(A/B)$ is maximum at a slightly higher aperture angle $\theta \approx 0.29\pi$.

F. Global post-measurement purity

The average state of the whole system after the previous local measurement at B is

$$\rho'_{AB} = r_+ \rho_{A/B_+} \otimes \Pi_+ + r_- \rho_{A/B_-} \otimes \Pi_- . \quad (38)$$

Its purity is then given by

$$\begin{aligned} P'_{AB} &= \text{Tr}(\rho'_{AB})^2 = r_+^2 P_{A/B_+} + r_-^2 P_{A/B_-} \quad (39) \\ &= \frac{1}{2} \{ p \cos(\theta - \phi) + q \cos(\theta + \phi) \}^2 \\ &\quad - 2pq \sin^2 \theta [1 + \cos(\theta + \phi) \cos(\theta - \phi)] . \quad (40) \end{aligned}$$

In contrast with Eq. (23), this global post-measurement purity cannot be greater than the original purity (5), in agreement with the general considerations of [13]:

$$P'_{AB} \leq P_{AB}, \quad (41)$$

with $P'_{AB} < P_{AB}$ for $\theta \in (0, \pi/2)$ and $pq > 0$. The difference $P_{AB} - P'_{AB}$ is just proportional to the S_2 information deficit [13],

$$I_2(A, B_{\phi}) = S_2(\rho'_{AB}) - S_2(\rho_{AB}) = 2(P_{AB} - P'_{AB}), \quad (42)$$

which is always non-negative. Eq. (39) shows that it can also be evaluated just with the conditional purities $P_{A/B_{\pm}}$, the initial purity P_{AB} and the probabilities r_{\pm} . Its minimum

$$I_2(A, B) = \text{Min}_{\phi} I_2(A, B_{\phi}) \quad (43)$$

which corresponds to *maximum* global post-measurement purity P'_{AB} , is proportional to the *geometric discord* [13, 20], also an indicator of discord-like non-classical correlations. It will then be non-zero for $\theta \in (0, \pi/2)$ and $pq \neq 0$, being maximum, like the quantum Discord, at an angle θ above $\pi/4$, as appreciated in Fig. 2.

The measurement angle ϕ maximizing P'_{AB} (and minimizing $I_2(A, B_{\phi})$) satisfies

$$\tan 2\phi = \frac{(p - q) \sin 2\theta}{pq + (1 - pq) \cos 2\theta}. \quad (44)$$

It is smaller than that maximizing $P_{A/B_{\phi}}$ (Eq. (25)). It can in fact be larger or smaller than θ , with $\phi \approx \theta - (1 - p) \cos^2 \theta \sin 2\theta$ for $p \rightarrow 1$. On the other hand, for $p \rightarrow 1/2$, $\phi \rightarrow \pi/2$ just for $\cos \theta \leq 1/\sqrt{3}$, i.e. $\theta > \theta_c \gtrsim 0.309\pi$, with $\phi \rightarrow 0$ for $\cos \theta > 1/\sqrt{3}$. Hence, for $p = 1/2$ a *sharp transition* from 0 to $\pi/2$ in the maximizing measurement angle of P'_{AB} , occurs at $\theta = \theta_c$ [13]. Such sharp transition becomes smoothed out for $p > q$, as seen in Fig. 2.

Since at fixed θ , the minimizing angle ϕ of (42) can differ from that minimizing the quantum discord, the behavior of (42) as a function of the measurement angle ϕ may become out of phase with that of the quantum discord, as will be appreciated in Fig. 5. In particular, for $p = q$ and $\theta < \theta_c$, (42) is minimum at $\phi = 0$, where $P_{A/B_{\phi}}$ is minimum and hence $D(A/B_{\phi})$ is maximum (as a function of ϕ). This difference is indicating the distinct meaning of the optimizing angles of $P_{A/B_{\phi}}$ and $D(A/B_{\phi})$ on one side, and $I_2(A, B_{\phi})$ on the other side. While the former chooses essentially the local direction associated with maximum correlation, the latter represents the direction of a least disturbing local measurement [13], which produces the smallest global purity decrease. Accordingly, differences can be significant for small aperture angles θ , where the latter will be closer to the z axis, but will decrease as θ increases, as appreciated in the bottom panel of Fig. 2. For $p = q$ they vanish in fact for $\theta > \theta_c$.

Let us finally remark that the direction \mathbf{k} in the Bloch sphere of B of the measurement minimizing (42) satisfies the standard eigenvalue equation [13, 20]

$$(J^T J + \mathbf{r}_B \mathbf{r}_B^T) \mathbf{k} = \lambda \mathbf{k}, \quad (45)$$

with λ the maximum eigenvalue, where $J_{\mu\nu} = \langle \sigma_{\mu}^A \otimes \sigma_{\nu}^B \rangle = C_{\mu\nu} + \langle \sigma_{\mu}^A \rangle \langle \sigma_{\nu}^B \rangle$. In the present situation Eq. (45) shows that \mathbf{k} lies in the xz plane, i.e., $\mathbf{k} = (\sin \phi, 0, \cos \phi)$, with ϕ satisfying Eq. (44). Actually, the maximizing ϕ is the smallest positive root of (44), the other root corresponding to the angle minimizing P'_{AB} (smallest eigenvalue of (45)).

III. EXPERIMENTAL VERIFICATION

A. Experimental setup

The experimental setup is depicted in Fig. 3. It can be divided in three stages. In the first part, used for state preparation, a LiIO3 nonlinear crystal cut for type-I phase-matching, is pumped by an horizontally polarized 405nm laser diode, that by means of spontaneous parametric down conversion (SPDC) produces pairs of twin photons with wavelength $\lambda = 810$ nm in the two-qubit polarization state $|VV\rangle$. A half-wave plate (HWP₁) is used to rotate the polarization of each photon to an arbitrary direction θ_L in the laboratory reference system, where $\theta_L = 0$ corresponds to vertically polarized photons. This angle defines the state $|\theta\rangle$ in the Bloch sphere through the relation $\theta = 2\theta_L$. In order to generate the mixed two-qubit states described by Eq. (1), we followed the idea presented in [38] switching HWP₁ between the two angles $\theta_L/2$ and $-\theta_L/2$ to obtain a mixture of the two desired polarizations with probabilities p and q .

In the second part of the setup, a local projective polarization measurement is done in one of the subsystems. To this end, a linear polarizer (P₁) in the path B, set at an angle ϕ_L or $\phi_L + \pi/2$ in the laboratory reference system, implements the action of the projector Π_+ or Π_- of Eq. (13) on the single qubit state. After that, the light is collected by the detector D_B. The detector is conformed by an iris that acts as spatial filter, and an interference filter centered at 810nm (10 nm bandwidth), followed by a lens that collects the light and focuses it in a multi mode optical fiber coupled to a photon counting module PerkinElmer SPCM-AQRH-13-FC. During the total time T that P₁ is set at the angle ϕ_L , D_B measures the number of single counts n_+ , and the same is done when P₁ is set at the complementary angle $\phi_L + \pi/2$ to register n_- . Then, the probability of measuring + or - along the direction ϕ (r_{\pm}) given in Eq. (14) is obtained as $n_{\pm}/(n_+ + n_-)$.

Finally, the third part of the set up is used to perform a complete single-qubit tomography on the subsystem A. An array of a quarter-wave plate (QWP), a half-wave plate (HWP₂), and a linear polarizer (P₂) in the path of the subsystem is used to project the polarization state onto the informational complete set of mutually unbiased basis [39, 40], before being detected by D_A. This detector consists of the same components than D_B, which was described above. The measurements are performed in coincidence, using the subsystem B as a trigger. In this way it is possible to reconstruct the conditional density matrix $\rho_{A/B=\pm}$ of the reduced state of A after obtaining the outcome \pm of the projective measurement along direction ϕ at B. Although these observables could be obtained by performing a conditional purity measurement, the used set up additionally allows to verify that the post-measurement local conditional state was of the form (16).

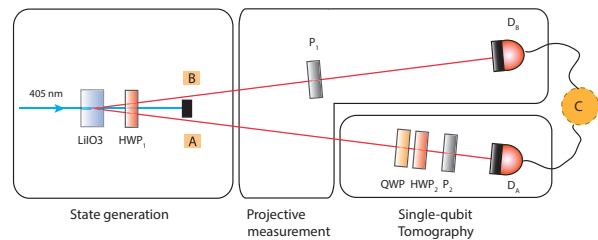


FIG. 3: Experimental setup used to the preparation of a mixed polarization two-qubits state, and characterization of the single-qubit state in A conditional to a projective measurement at B. QWP: quarter-wave plate; HWP: half-wave plate; P: linear polarizer; D: single photon detector.

B. Results

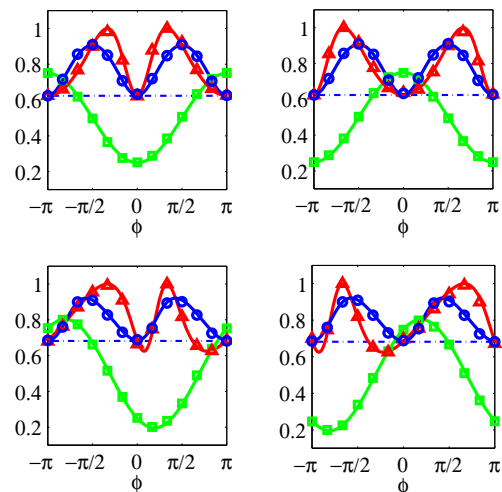


FIG. 4: (Color online) Experimental results obtained from each projective measurement described by Π_{\pm} . It shows the purity of the state A after obtaining the result - (left panels) or + (right panels) at B, $P_{A/B=\pm}$ (Eq. (18)) (red triangles), and the probability to obtain this result, r_{\pm} (green squares). Additionally, each graphic shows the average conditional purity $P_{A/B,\phi}$, Eq. (21) (blue circles). In all cases the initial state is a two-qubit state with $\theta = \pi/3$. For the top panels $p=0.5$ and for the bottom panels $p=0.7$. Solid lines correspond to the theoretical values for these measures as a function of ϕ . The dashed line indicates the measured value of the local purity P_A in the initial state before conditional measurement.

As mentioned above, the first section of the experimental setup generates a two-photon field in the polarization state given by Eq. (1). In order to validate the generation process, a previous complete tomography [41] for different mixed two-qubit states was done. Afterwards, maximum likelihood technique (ML) was applied to obtain the best state estimation consistent with the requirements of a physical state [42]. We quantified the quality of the preparation process by means of the fi-

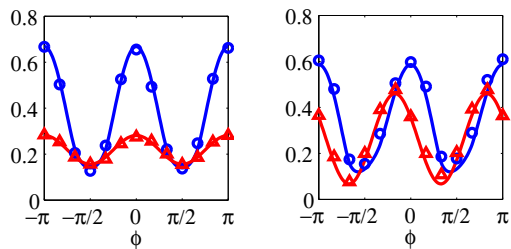


FIG. 5: (Color online) Experimental results obtained from each projective measurement described by Π_{\pm} . The minimum of the blue line (circles) is the value of the quantum discord while the minimum of the red line (triangles) is the value of geometric discord (minimum global purity difference). The initial state is a two qubit state corresponding to $\theta = \pi/3$ with $p=0.5$ (left panel) and $p=0.7$ (right panel). Solid lines correspond to the theoretical values for these measures as a function of the measurement angle ϕ .

delity $F \equiv \text{Tr}(\sqrt{\sqrt{\sigma}\rho\sqrt{\sigma}})$ between the density matrix of the state intended to be prepared, σ , and the density matrix of the state actually prepared and reconstructed by tomography, ρ . In all cases, fidelities $F > 0.98$ for the initial state ρ_{AB} were obtained. After this previous characterization we performed the projective measurements and the conditional one-qubit tomography implemented in the second and third parts of the setup (Fig. 3). The post measurement state $\rho_{A/B_{\pm}}$ in Eq. (16) was obtained after applying the ML technique to the experimental results. The plots in Fig. 4 show the probabilities for the projective measurements r_{\pm} and the conditional purities $\text{Tr}\rho_{A/B_{\pm}}^2$ for two different initial states together with the theoretical predictions given by Eqs. (14) and (18). Additionally, we plot the average conditional purity $P_{A/B_{\phi}}$ which was obtained from the experimental results as $r_+P_{A/B_+} + r_-P_{A/B_-}$ and theoretically as $1 - 2pq\gamma \sin^2 \theta$ (Eq. (21)). In Fig. 5 we plot the experimental and theoretical results for $D(A/B)$ and $I_2(A, B_{\phi})$, whose minimum values as a function of the projective measurement Π_{ϕ} correspond to the quantum discord and the geometric discord respectively. As follows from Sec. II E and Sec. II F both quantities can be evaluated from the purities P_{AB} , P_A , and $P_{A/B_{\pm}}$. For this purpose, the density matrix of the reduced state ρ_A was obtained in a similar way to $\rho_{A/B_{\pm}}$ but considering the single counts in D_A without taking in account the results in D_B .

IV. CONCLUSIONS

We have examined in full detail the quantum correlation properties of the two-parameter mixed states (1), characterized by an aperture angle and a probability or weight p . Such states arise naturally as reduced two-spin states of spin 1/2 chains, either at the mean field approximation level or exactly in the vicinity of the factorizing field, and can be easily generated by photonic qubit states in a linear-optics architecture. We have derived simple exact analytical expressions for the conditional purity of one of the qubits after a local measurement on the other qubit, including its maximum average. We have then derived a simple exact analytical expression for the quantum discord of the state, which unveils a simple connection of the latter with the previous maximum average conditional purity, valid for the present states. This result allows a straightforward experimental evaluation of the quantum discord through a conditional single photon purity measurement. The global post-measurement purity and its maximum were as well analytically evaluated and compared with the previous measures. The experimental results showed a remarkable agreement with the theoretical predictions. The analysis shows that the form of the reduced state of the unmeasured photon A remains unchanged after a remote measurement on photon B , although selection of the measurement angle allows full control of the probabilities characterizing this reduced state, including pure and maximally mixed limits. At the same time, due to the non-orthogonality of the states involved these probabilities do affect the eigenstates of the conditional reduced states, and any local measurement does affect the average post-measurement global state. Possible applications to cryptography and metrology are currently under investigation.

V. ACKNOWLEDGMENTS

The authors acknowledge support from CIC (RR) and CONICET (LR, JJMV, NG, NC, CI, SL) of Argentina. L.R. thanks the Institut für Gravitationsphysik and Leibniz Universität Hannover for kind hospitality. This work was supported by UBACyT 20020130100727BA, CONICET PIP 112201101-00902, CONICET PIP 112200801-03047, and ANPCYT PICT 201002179 (Argentina).

-
- [1] M. Nielsen, and I.L. Chuang, *Quantum Computation and Quantum Information* (Cambridge Univ. Press, Cambridge, UK, 2000).
[2] C.H. Bennett, et al. Phys. Rev. Lett. **70**, 1895 (1993).
[3] R. Jozsa and N. Linden, Proc. R. Soc. London Ser. A **459**, 2011 (2003); G. Vidal, Phys. Rev. Lett. **91**, 147902 (2003).
[4] R. Raussendorf and H. J. Briegel, Phys. Rev. Lett. **86**,

- 5188 (2001); R. Raussendorf, D. E. Browne, and H. J. Briegel, Phys. Rev. A **68**, 022312 (2003).
[5] B. Schumacher, Phys. Rev. A **51**, 2738 (1995).
[6] R.F. Werner Phys. Rev. A **40**, 4277 (1989).
[7] K. Modi et al, Rev. Mod. Phys. **84**, 1655 (2012).
[8] H. Ollivier and W.H. Zurek, Phys. Rev. Lett. **88**, 017901 (2001).
[9] L. Henderson and V. Vedral, J. Phys. A **34**, 6899 (2001).

- [10] V. Vedral, Phys. Rev. Lett. **90**, 050401 (2003).
- [11] A. Datta, A. Shaji, C.M. Caves, Phys. Rev. Lett. **100**, 050502 (2008).
- [12] A. Streltsov, H. Kampermann, and D. Bruß, Phys. Rev. Lett. **106**, 160401 (2011); M. Piani et al, Phys. Rev. Lett. **106**, 220403 (2011).
- [13] R. Rossignoli, N. Canosa, L. Ciliberti, Phys. Rev. A **82** 052342 (2010); Phys. Rev. A **84** 052329 (2011).
- [14] L. Roa, J. C. Retamal, and M. Alid-Vaccarezza, Phys. Rev. Lett. **107**, 080401 (2011).
- [15] S. Pirandola, Scientific Reports **4**, 6956 (2014).
- [16] D. Girolami, T. Tufarelli, and G. Adesso, Phys. Rev. Lett. **110**, 240402 (2013).
- [17] N. Gigena, R. Rossignoli, J. Phys. A **47** 015302 (2014); Phys. Rev. A **90**, 042318 (2014).
- [18] R. Filip, Phys. Rev. A **65** 062320 (2002); H. Nakazato et al, Phys. Rev. A **85** 042316 (2012); T. Tanaka et al, Phys. Rev. A **87** 012303 (2013); K. Bartkiewicz, K. Lemr, and A. Miranowicz, Phys. Rev. A **88**, 052104 (2013).
- [19] T. A. Brun, Quantum Information and Computation **4**, 401 (2004); F. A. Bovino, et al, Phys. Rev. Lett. **95**, 240407 (2005); J. Du, et al, Phys. Rev. A **74** 042319 (2006); R. B. A. Adamson, L. K. Shalm, and A. M. Steinberg, Phys. Rev. A **75**, 012104 (2007).
- [20] B. Dakić, V. Vedral, and Č. Brukner, Phys. Rev. Lett. **105**, 190502 (2010).
- [21] A. Orioux, J. Boutari, M. Barbieri, M. Paternostro and P. Mataloni, Sci. Rep. **4**, 7184 (2014).
- [22] Xiao-song Ma et. al, Sci. Rep. **4**, 3583 (2014).
- [23] J. Kurmann, H. Thomas, and G. Müller, Physica A **112**, 235 (1982).
- [24] R. Rossignoli, N. Canosa and J.M. Matera, Phys. Rev. A **77**, 052322 (2008); Phys. Rev. A **80**, 062325 (2009).
- [25] N. Canosa, R. Rossignoli and J.M. Matera, Phys. Rev. B **81**, 054415 (2010).
- [26] L. Ciliberti, R. Rossignoli, and N. Canosa, Phys. Rev. A **82**, 042316 (2010).
- [27] A. Boette, R. Rossignoli, N. Canosa, J.M. Matera, Phys. Rev. B **91**, 064428 (2015).
- [28] D. C. Burnham and D. L. Weinberg Phys. Rev. Lett. **25**, 84 (1970)
- [29] L. Mandel and E. Wolf, *Optical coherence and quantum optics* (Cambridge University Press, New York, 1995).
- [30] H. Wehrl, Rev. Mod. Phys. **50**, 221 (1978).
- [31] N. Canosa and R. Rossignoli, Phys. Rev. Lett. **88**, 170401 (2002).
- [32] R. Bhatia, *Matrix Analysis* (Springer-Verlag, New York, 1997).
- [33] M.A. Nielsen and J. Kempe, Phys. Rev. Lett. **86**, 5184 (2001).
- [34] R. Rossignoli, N. Canosa, Phys. Rev. A **67**, 042302 (2003); R. Rossignoli, N. Canosa, Phys. Rev. A **66**, 042306 (2002).
- [35] S. Hill, W.K. Wootters, Phys. Rev. Lett. **78** 5022 (1997); W.K. Wootters, Phys. Rev. Lett. **80**, 2245 (1998).
- [36] M. Koashi and A. Winter, Phys. Rev. A **69**, 022309 (2004).
- [37] D. Cavalcanti et al, Phys. Rev. A **83** 032324 (2011); V. Madhok and A. Datta, Phys. Rev. A **83** 032323 (2011). F.F. Fanchini et al, Phys. Rev. A **84** 012313 (2011).
- [38] E. Amsellem and M. Bourennane, Nat. Phys. **5**, 748 (2009)
- [39] I.D. Ivanovic, J. Phys. A **14**, 3241 (1981).
- [40] W. K. Wootters and B. D. Fields, Ann. Phys. **191**, 363 (1989).
- [41] D.F.V. James, P.G. Kwiat, W.J. Munro, and A.G. White, Phys. Rev. A **64**, 052312 (2001).
- [42] J. Fiurášek, Phys. Rev. A **64**, 024102 (2001).